Chemical Physics Letters 806 (2022) 140052

Contents lists available at ScienceDirect

Chemical Physics Letters

journal homepage: www.elsevier.com/locate/cplett

Density functional theory investigation on structural, mechanical, electronic and vibrational properties of Heusler alloys $AlXIr_2$ (X = Co, Cr, Cu, Fe and Zn)

Ahmet Iyigör [a], Selgin Al [b,*], Nihat Arikan [c]

[a] Department of Machine and Metal Technologies, Kirsehir Ahi Evran University, Kirsehir, Turkey
[b] Department of Environmental Protection Technologies, Izmir Democracy University, Izmir, Turkey
[c] Department of Medical Services and Techniques, Osmaniye Korkut Ata University, Osmaniye, Turkey

ARTICLE INFO

Keywords:
Full-Heusler
Dynamical stability
Phonon
Mechanic properties

ABSTRACT

This study focuses on the detailed investigation of full-Heusler $AlXIr_2$ (X = Co, Cr, Cu, Fe and Zn) alloys. A first-principal plane-wave pseudopotential method based on density functional theory is adopted. The quantum-espresso package combined with the generalized gradient approach is used to reveal the structural, electronic, magnetic, mechanical and lattice dynamic properties of full-Heusler $AlXIr_2$ (X = Co, Cr, Cu, Fe and Zn) alloys. The elastic constants are used to determine elastic stabilities of alloys based on Born criteria. The analysis showed that all alloys are elastically stable. Further detailed analysis has been carried out to reveal mechanical properties. It is found that all alloys are ductile and anisotropic. The electronic band structures are also obtained. All alloys except for $AlCrIr_2$ are found to be metallic. $AlCrIr_2$ has half-metallic nature. In addition, $AlCrIr_2$, $AlFeIr_2$ and $AlCoIr_2$ has shown magnetic properties. The phonon spectra and density of states are investigated to examine dynamical stability. It is seen that all alloys exhibit dynamical stability due to having positive phonon frequencies.

1. Introduction

Friedrich Heusler reported the discovery of both half and full Heusler alloys in 1903 which made it possible to form ferromagnetic compounds from non-ferromagnetic components [1]. Heusler alloys are important materials which have received considerable theoretical and experimental interest, including a wide range of materials with hundreds of fundamental combinations, and have been known for over 100 years. Half-metallic ferromagnetic (HMF) materials have attracted lots of attention in applications of spintronic devices such as magnetic sensors [2,3], memory storages [4–6], spin filters [7], spin valves [8], tunnelling magnetoresistance (TMR) phenomena [9] and electromechanical [10] applications. Since the prediction of NiMnSb. [11] as the first half-metallic ferromagnet, many materials have been investigated both theoretically and experimentally to obtain HMF properties. In these types of materials, the two spin bands behave differently, that is, at the Fermi energy (E_F) level, the majority spin band shows typical metallic behaviour, and the minority spin band displays an energy gap. Thus, they result in 100% spin polarization which are important for the efficiency of spintronic devices. Although many theoretical and experimental studies [3,12,13] have been conducted on Heusler alloys to demonstrate their use as multifunctional materials to date, most of all possible chemical compositions still wait for to be explored.

Considering its important applications in spintronic devices, memory storage devices, tunnelling magnetic resonance (TMR) and giant magnetoresistance (GMR), Ir-based Heusler alloys have attracted the attention of numerous researchers in terms of their structural stability and the possible half-metallic properties. However, there are limited experimental and theoretical studies on Ir-based Heusler alloys. Prakasha and Kalpana [14] calculated magnetic and electronic band properties of full Heusler alloys Ir_2YSi (Y = Sc to Ni) in the $L2_1$ and X_a (Hg_2CuTi structure) phases using full-potential linearized augmented plane wave method (FP-LAPW) based on density functional theory (DFT). Also, the crystal structural and magnetic properties of IrMnGa, IrMnSn, IrMnSb and IrMnAl alloys in both $C1_b$ and $L1_2$ phases were investigated by Matsumoto *et al.* [15,16]. The electronic band structure, mechanical, thermodynamic properties of Ir_2ScAl alloy were studied along with the lattice dynamic properties using density functional perturbation theory

* Corresponding author.
E-mail address: selgin.al@idu.edu.tr (S. Al).

https://doi.org/10.1016/j.cplett.2022.140052
Received 1 July 2022; Accepted 10 September 2022
Available online 16 September 2022
0009-2614/© 2022 Elsevier B.V. All rights reserved.

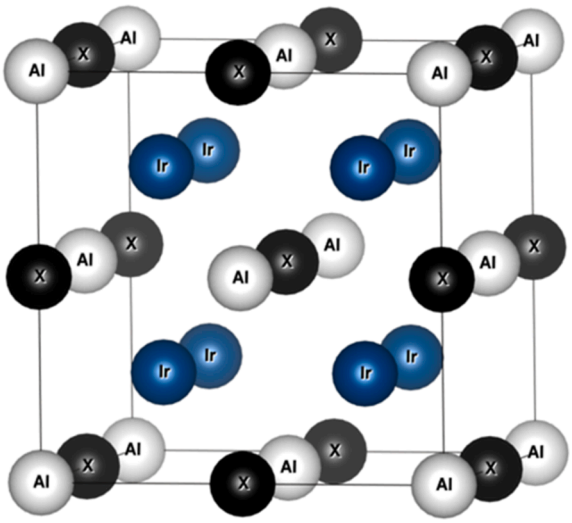

Fig. 1. Crystal structures of $AlXIr_2$ (X = Co, Cr, Cu, Fe and Zn).

(DFPT) implemented in quantum-espresso code [17]. From the calculated elastic and lattice dynamic properties, it has been shown that the Ir_2ScAl alloy in the $L2_1$ phase is mechanically and dynamically stable. The magnetic, elastic, and electronic properties of full-Heusler Ir_2MnSi alloy were studied within the framework of DFT [18]. In another study, structural, electronic, magnetic, and optical properties of Ir_2ScZ (Z = Si, Ge, Sn) alloys investigated [19]. It is reported that their high Curie temperatures, and their half-metallic properties under stress of the Heusler compounds can be used efficiently to make optical devices such as solar and photovoltaic cells, and they are good candidates for use in spintronic devices and spin valves.

In this work, we are focused on investigating $AlXIr_2$ (X = Co, Cr, Cu and Zn) full-Heusler alloys, we have presented detailed explanations about the mechanical and lattice dynamic properties of these alloys. Although few theoretical advances are likely to be made for $AlXIr_2$ (X = Co, Cr, Cu, Fe and Zn) alloys, many of their physical properties are still not fully determined. At this point, only formation enthalpies and lattice constants were calculated for these alloys using theoretical calculations by Gilleßen [20].

The phonon properties of the materials are an important parameter to understand the physical nature of solids such as thermal expansion, specific heat, electron–phonon interaction, heat conduction, and phase transition. The full phonon and mechanical properties of $AlXIr_2$ (X = Co, Cr, Cu, Fe and Zn) full-Heusler alloys have not been studied using any experimental or theoretical method based on the existing data. This study aims to investigate the structural, electronic, magnetic, thermodynamic, and vibrational properties of $AlXIr_2$ (X = Co, Cr, Cu, Fe and Zn) full-Heusler alloys using DFT and Quantum-espresso code. We also performed the phonon spectra and their total and partial density using the ab initio linear-response approach.

2. Method

Ab initio computations were executed for $AlXIr_2$ (X = Co, Cr, Cu, Fe and Zn) alloys using first principles plane wave pseudopotential method implemented in Quantum Espresso code [21,22]. We used ultra-soft pseudo-potentials to calculate the interaction between the nuclei, valence electron, and the core electrons. The electronic exchange correlation potentials were treated by using the generalized slope approximation (GGA) parameterized by Perdew, Burke, and Ernzerhof (PBE) [23]. The cut-offs for wave functions and charge density were evaluated to be 40 Ry and 400 Ry, respectively. Brillouin-zone integrations were performed using 10 × 10 × 10 k points. It was carried out using the smearing technique [24] with the smearing parameter as σ = 0.02 Ry for integration up to the Fermi surface. Next computing the solutions of Kohn-Sham equations, the lattice dynamic properties for $AlXIr_2$ were evaluated by employing a linear-response technique [25,26] based on the density-functional theory. The dynamical matrices at arbitrary wave vectors were carried out on a 4x4x4 q-point mesh and a Fourier deconvolution was applied on this mesh to calculate the complete phonon dispersions and vibrational density of states.The elastic properties (G and E) were obtained from the Hill value, which is a geometric mean of the Voigt and Reuss values using energy-strain method implemented in thermos-pw code [21]. Other relevant elastic moduli can also be obtained using three elastic constants (C_{ij}) for the cubic system.

Table 1
The calculated lattice constants (a, Å), total magnetic moment (M_t, μ_B), Bulk modulus (B, GPa), Shear Modulus (G, GPa), Young Modulus (E, GPa), B/G ratio, Poisson's ratios (σ) and elastic constants (C_{11}, C_{12}, C_{44}, GPa) of $AlXIr_2$ (X = Cr, Fe, Co, Cu and Zn).

Materials	*References*	a_0 (Å)	M_t (μ_B)	B (GPa)	G (GPa)	E (GPa)	B/G	σ	C_{11} (GPa)	C_{12} (GPa)	C_{44} (GPa)	C_P=(C_{12}-C_{44})
$AlCrIr_2$	This work	6.056	3.04	243.582	60.909	164.261	3.999	0.34	257.687	236.529	155.969	80.56
	[39]	6.061	2.93									
	[40]	6.069	3.00									
	[41]	5.964	3.00	270.926								
$AlFeIr_2$	This work	6.057	4.34	228.837	85.608	228.051	2.673	0.33	291.528	197.491	127.781	69.71
	[39]	6.024	4.27									
	[42]	6.043	4.34									
	[40]	6.042	4.30									
$AlCoIr_2$	This work	6.017	2.94	236.829	91.180	242.129	2.597	0.32	304.414	203.037	135.025	68.012
	[39]	5.963	–									
	[42]	–	–									
	[40]	6.003	2.89									
$AlCuIr_2$	This work	6.033	0.00	226.144	101.116	263.775	2.236	0.30	306.438	185.997	143.091	42.906
	[39]	5.991	0.00									
	[42]	–	–									
	[40]	6.012	0.00									
$AlZnIr_2$	This work	6.058	0.00	221.972	110.446	284.199	2.009	0.28	345.657	160.130	124.100	36.03
	[39]	6.048	0.00									
	[42]	6.055	0.00									
	[40]	6.056	0.00									

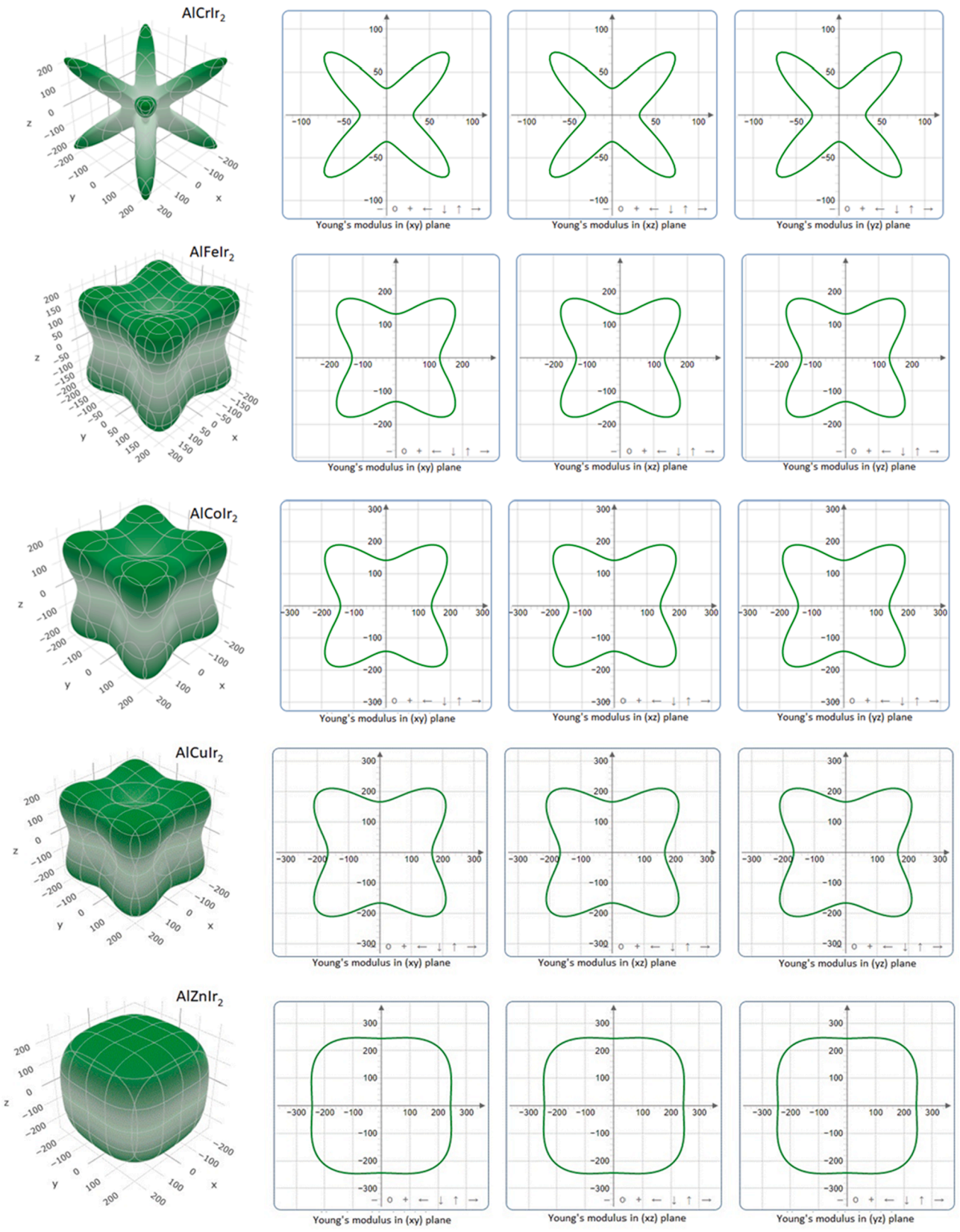

Fig. 2. 2D curves of Young Modulus of $AlXIr_2$ (X = Cr, Fe, Co, Cu and Zn).

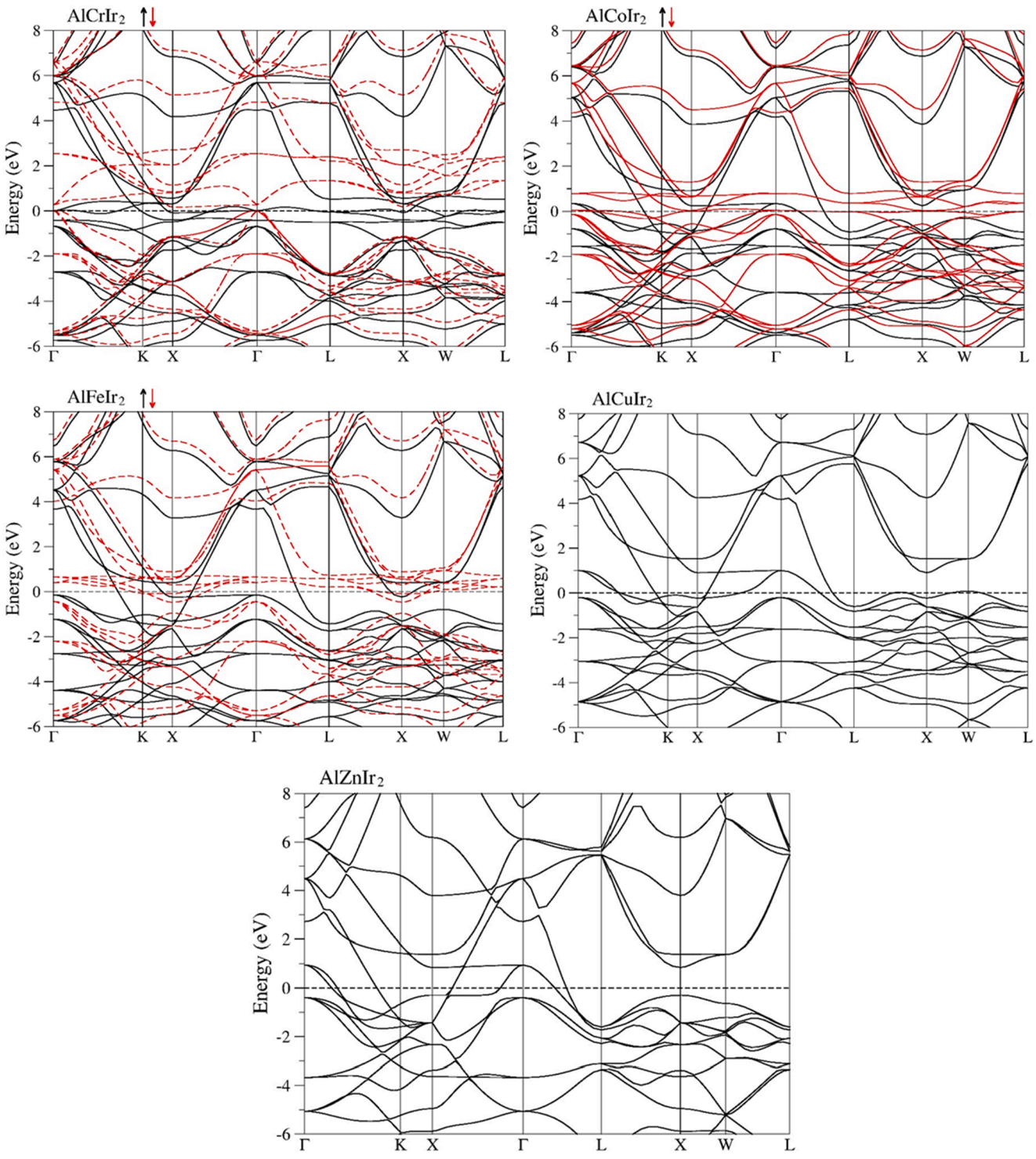

Fig. 3. Electronic band structures of $AlXIr_2$ (X = Cr, Fe, Co, Cu and Zn).

3. Results and discussion

$AlXIr_2$ alloys from the full-Heusler family crystallize in the $L2_1$ phase with the space group Fm $\overline{3}$ m (no.225) as shown in Fig. 1. The equilibrium lattice constants are calculated and presented in Table 1. Firstly, total energies are calculated as a function of changing unit cell volume around the equilibrium volume where energy-volume data is obtained. Then this data is fitted the Murnaghan's equation of state. The equilibrium volume is determined by finding the minimum energy level where the volume is called optimised equilibrium volume and the energy is called ground state energy. The obtained equilibrium lattice constants and bulk modulus are given in Table 1 and compared to the available existing data. It is seen that the obtained lattice constants of materials are in a good agreement with the available data.

In general, the elastic properties of materials indicate their resistance to volume change under an external pressure. It also gives information about the nature of forces in solid materials and hardness, stiffness and stability of materials [27,28]. There are three independent elastic constants for a single cubic crystal which are calculated using the general approach [29,30]. The calculations are based on an assessment of

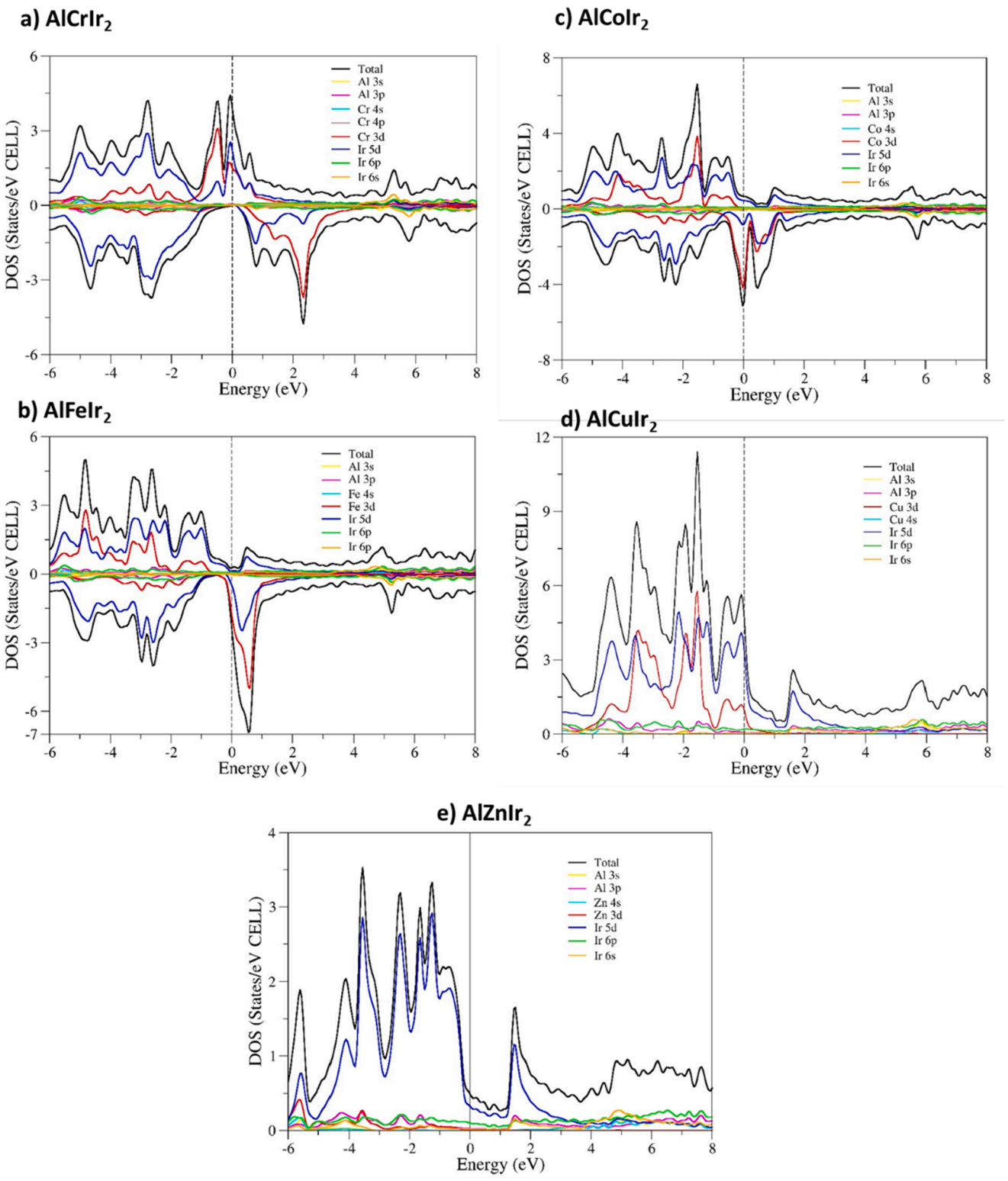

Fig. 4. Total and partial density of states of $AlXIr_2$ (X = Cr, Fe, Co, Cu and Zn).

changes in total energy values resulting from changes in applied strain. The elastic constants of alloys are presented in Table 1. For a stable material, these elastic constants should satisfy the Born stability criteria [31,32];

$$(C_{11} - C_{12}) > 0, C_{11} > 0, C_{44} > 0, (C_{11} + 2C_{12}) > 0 \quad (1)$$

Equation (1) is also deducted as;

$$C_{12} < B < C_{11} \quad (2)$$

As can be deduced from Table 1 that, the elastic constants of alloys fulfil the requirements given in equation (1) and (2). This indicates that all alloys are elastically stable. It is stated that C_{11} indicates the unidirectional compression induced along principal crystallographic directions [33]. As it is noticed from Table 1 that The C_{11} values of alloys

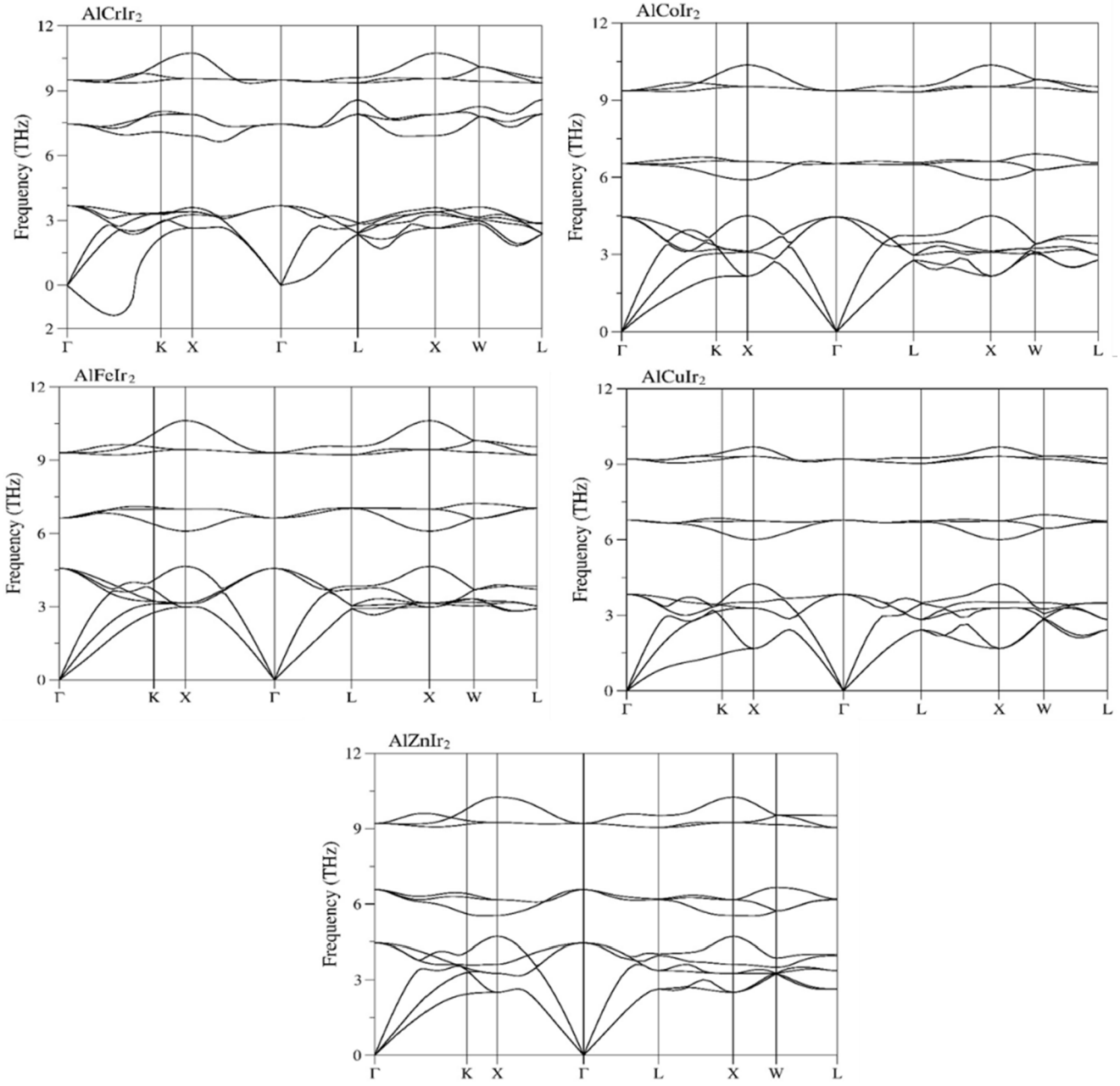

Fig. 5. Phonon dispersion curves of $AlXIr_2$ (X = Cr, Fe, Co, Cu and Zn).

are much higher than the C_{44} values which implies that these alloys will show stronger resistance to unidirectional compression than the pure shear deformation. In addition, the large bulk modulus *B* describes larger deformation resistance against the change in volume under external pressure. Thus, the deformation resistance of materials can be classified as $AlCrIr_2 > AlCoIr_2 > AlFeIr_2 > AlCuIr_2 > AlZnIr_2$.

Pettifor [34] stated that Cauchy pressure $C_{12} - C_{44}$ can provide information about the nature of angular atomic bonding in alloys which also depicts materials' ductility and brittleness. If the Cauchy pressure is negative, the material has directional bonding with angular or covalent character and brittle nature. The larger negative value of Cauchy pressure indicates added directional character whereas a positive Cauchy pressure points out metallic character and ductile nature. Based on the Cauchy pressures of alloys given in Table 1, it can be said that all alloys show metallic character and ductile nature.

Ductility and brittleness of alloys can also be examined by using B/G ratio and Poisson's ratio. The ratio of B/G which is also called Pugh's criteria [35,36] defines materials ductility and brittleness. If B/G ratio is greater than 1.75, the material is ductile, otherwise it is brittle. As the materials B/G ratios are greater than 1.75, all alloys are found to be ductile in nature. Frantsevich et al. [37] stated that Poisson's ratio can distinguish ductility and brittleness of materials by the ratio of 0.26. The materials with the Poisson's ratio less than 0.26 are classified as brittle and greater than 0.26 ratio are classified as ductile. All $AlXIr_2$ alloys have Poisson' ratio greater than 0.26 which endorses ductile nature. Poisson's ratio also provides information about bonding natures of the materials. Covalently bonding materials tend to have Poisson's ratio around 0.1 whereas ionic materials have Poisson's ration around 0.25. The typical value for metals is reported as 0.33 [38]. In our study, the alloys Poisson's ratios are found to be around 0.33 which signifies metallic characteristics of materials.

Another important parameter which is collected by using elastic constants is that A, anisotropy factor. Anisotropy factor is especially critical for high-tech applications since it helps to predict micro-cracks

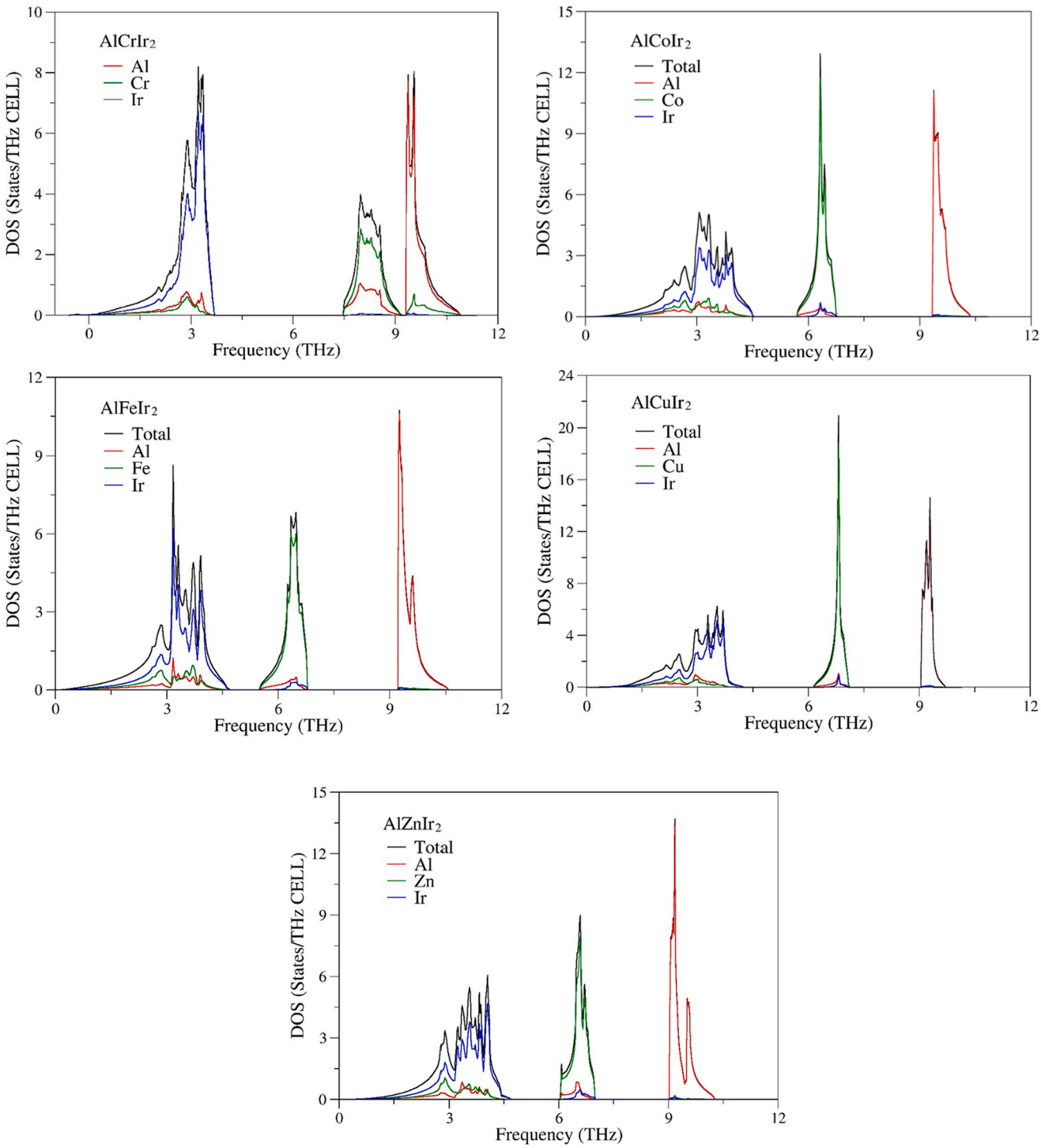

Fig. 6. Phonon density of states of $AlXIr_2$ (X = Cr, Fe, Co, Cu and Zn).

in solids and measures the durability of materials. It measures intensity of property in different directions. The anisotropy factors of alloys are calculated the elastic constants ($A = 2C_4/C_{11}\text{-}C_{12}$). The obtained anisotropy factors are 14.743 for $AlCrI_2$, 2.717 for $AlFeI_2$, 2.663 for $AlCoI_2$, 1.188 for $AlCuI_2$ and 1.337 for $AlZnI_2$. In the case of unity, the anisotropy factor equals to 1. The computed anisotropy factors of alloys are higher than 1 which indicates anisotropic nature of alloys.

The Shear modulus, G, describes material's resistance against shape change due to a shear strain. Based on our calculations, $AlZnIr_2$ has higher Shear modulus than other alloys, indicating that $AlZnIr_2$ has higher hardness among them and $AlCrIr_2$ has lowest value of Shear modulus, suggesting that $AlCrIr_2$ has the lowest hardness. Young modulus, E, defines the ratio of stress to strain and it is a measure of stiffness solids [43]. The highest value of Young modulus demonstrates highest stiffness. Based on our calculations, $AlZnIr_2$ has the highest stiffness and $AlCrIr_2$ has the lowest stiffness among the studied alloys. Recently, observation of anomalous materials has led researchers to explore anisotropy of elastic constants due to stress and strain. If the material is loaded unusually in tension, it tends to extend in this direction which results in deformation. Therefore, the 2D changes of Young modulus along the planes are obtained and presented in Fig. 2. The plots are constructed along xy, yz and xz planes. The projections of planes are

also presented. The isotropy of the alloy is shown by circular, deviation from that suggests anisotropy. As can be seen from Fig. 2 that $AlCrIr_2$ displays the highest anisotropy and $AlZnIr_2$ shows the lowest anisotropy. The degree of deformation in $AlCrIr_2$ is higher at all directions. From $AlCrIr_2$ to $AlZnIr_2$ the circularity increases in all directions, implying that isotropy increases as atomic numbers of the alloys increase.

The total magnetic moment of each alloy is also computed with the help of GGA and presented in Table 1. The total magnetic moment of $AlCrIr_2$ is found as 3.04 μ_B and 4.34 μ_B for $AlFeIr_2$ and 2.94 μ_B for $AlCoIr_2$. $AlCuIr_2$ and $AlZnIr_2$ has shown zero magnetic moment. Based on that, it can be said that $AlFeIr_2$, $AlCoIr_2$ and $AlCrIr_2$ are ferromagnetic materials. Also, as half-metallic ferro magnet $AlCrIr_2$ follows the Slater-Pauling rule, $M_t = N_v$-24, where N_v presents the number valence electrons for $AlCrIr_2$ in the unit cell [44]. The N_v is 27 for $AlCrIr_2$, thus the total magnetic moment is calculated as 3 μ_B using Slater-Pauling rule which is close to value that is obtained using GGA.

In order to predict electronic properties of full-Heusler $AlXIr_2$ (X = Co, Cu, Fe, Ni and Zn) alloys, the electronic band structures and total and partial density of states are calculated using GGA approximation and presented in Figs. 3 and 4. The Fermi energy level is set to 0 eV. The partial density of states is calculated to see contributions of atomic states near Fermi level. The band structures for spin up and spin down states for $AlCrI_2$, $AlCoIr_2$ and $AlFeIr_2$ are presented in both figures. It is seen from Fig. 3 that an overlap between the conduction and valence band exists for spin up states for $AlCrIr_2$, indicating a metallic nature for this state whereas a band gap of 0.22 eV is seen for spin down state, suggesting a semiconducting channel for this state. Thus, $AlCrIr_2$ reveals a half-metallic character. $AlCoIr_2$ and $AlFeIr_2$ spin up and spin down states overlap with each other, suggesting a metallic character for these alloys. Also, no band gap is seen in the band structures of$AlCuIr_2$ and $AlFeIr_2$ near Fermi energy level which confirms metallic characteristics for these alloys, too.

In order to determine the contributions of each orbital of an atom partial density of states are plotted in Fig. 4. The half-metallic character can be seen for spin down states of $AlCrIr_2$ as there is a band gap around Fermi energy level as valence and conduction band overlap in spin up states. It is clear from Fig. 4 that, the main contributions come from d states of Cr and Ir atoms to the total DOS for $AlCrIr_2$. The spin up and spin down states of $AlCoIr_2$ and $AlFeIr_2$ is also shown in Fig. 4. It is seen that d-states of spin up and spin down channels for both alloys overlap, suggesting a metallic character for these alloys. The contribution to the total DOS comes from the d-states of Co and Ir atoms for $AlCoIr_2$ as it comes from Fe and Ir atoms for $AlFeIr_2$. There is no band gap is seen for $AlCuIr_2$ and $AlZnIr_2$, indicating a metallic character. Ir-5d states contributes to the total DOS mainly with a little contribution from Cu-3d states for $AlCuIr_2$.

The phonon and phonon density of states of alloys are plotted in Figs. 5 and 6 along the high symmetry directions in the Brillouin zone. The phonon characteristics are important due to determining structural stability, vibrational and thermal properties. The alloys in this study have 4 atoms in their unit cell, corresponding to the 12 phonon modes. The lowest 3 phonon modes are acoustic modes which are the result of coherent lattice atoms motions outside of their equilibrium positions. The other 9 phonon modes are optic phonon modes. The frequency of acoustic modes provides information about the dynamical stability. Since the acoustic phonon modes have zero frequency at the Γ point, it can be said that all alloys have dynamical stability. In addition, there is no negative phonon frequencies are observed in phonon densities of alloys which also implies dynamical stability. The dynamical stability suggests no net force effecting the atoms; thus, the atoms are decisive and the alloys are dynamically stable.

The upper optical phonon modes frequencies are not zero at the Γ point. The optical modes give information about optical properties of materials. There is no phonon gap between the lower optical modes and acoustic modes of alloys. This results in a decrease in thermal conductivity of alloys due to a strong optical-acoustic phonon scattering [45]. The total and partial density of alloys is shown in Fig. 6 and can be divided into 3 parts as acoustic, lower and upper optical modes. It is seen from DOS that Ir atom mainly contributes to the acoustic phonon modes for all alloys. Lower optical phonon modes are contributed by all atoms whereas the upper optical phonon modes are contributed by Al atom due to being the lightest atom.

4. Conclusions

This study investigates structural, elastic, electronic, magnetic and vibrational properties of $AlXIr_2$ (X = Cr, Fe, Co, Cu and Zn) alloys using density functional theory. The computed lattice constants of alloys are in a well agreement with the available data. The detailed analysis of elastic constants and phonon properties indicates mechanical and dynamical stability of all alloys. All alloys are found to be ductile and elastically anisotropic. The analysis of electronic band structures of alloys reveals that $AlCrIr_2$ has a half-metallic character and other alloys have metallic character. Also, the alloys Poisson's ratios are found to be around 0.33 which signifies metallic characteristics of materials. The total magnetic moment of each material is also computed with the help of GGA. The total magnetic moment of $AlCrIr_2$ is found as 3.04 μ_B and 4.34 μ_B for $AlFeIr_2$ and 2.94 μ_B for $AlCoIr_2$. $AlCuIr_2$ and $AlZnIr_2$ has shown zero magnetic moment. The acoustic phonon modes have zero frequency at the Γ point; thus all alloys have dynamical stability. In addition, there is no negative phonon frequencies are observed in phonon densities of alloys which also implies dynamical stability. The properties of these alloys suggest that they can be good candidates for their future practical thermoelectric and spintronic applications.

Funding

There is no funding received for this study.

Data availability

The data is available from the corresponding author on reasonable request.

Declaration of Competing Interest

The authors declare that they have no known competing financial interests or personal relationships that could have appeared to influence the work reported in this paper.

References

[1] F. Heusler, Über magnetische manganlegierungen, J Verhandlungen der Deutschen Physikalischen Gesellschaft 5 (1903) 219.
[2] S. Berri, D. Maouche, M. Ibrir, B. Bakri, Electronic structure and magnetic properties of the perovskite cerium manganese oxide from ab initio calculations, J. Mater. Sci. Semicond. Process. 26 (2014) 199–204.
[3] F. Hosseinzadeh, A. Boochani, S.M. Elahi, Z. Ghorannevis, GdPtBi Heuslerene: mechanical stability, half-metallic, magneto-optic, and thermoelectric properties by DFT, Phil. Mag. 102 (10) (2022) 887–901.
[4] Y. Sokolovskaya, O. Miroshkina, D. Baigutlin, V. Sokolovskiy, M. Zagrebin, V. Buchelnikov, A.T. Zayak, A ternary map of Ni–Mn–Ga Heusler alloys from ab initio calculations, J. Met. 11 (6) (2021) 973, https://doi.org/10.3390/met11060973.
[5] M. Çanlı, E. Ilhan, N. Arıkan, First-principles calculations to investigate the structural, electronic, elastic, vibrational and thermodynamic properties of the full-Heusler alloys X_2ScGa (X= Ir and Rh), J. Mater. Today Commun. 26 (2021), 101855.
[6] J. Atulasimha, S. Bandyopadhyay, Nanomagnetic and spintronic devices for energy-efficient memory and computing, John Wiley & Sons. 2016.
[7] A. Bsiesy, Spin injection into semiconductors: towards a semiconductor-based spintronic device, J Comptes Rendus Physique 6 (9) (2005) 1022–1026.
[8] R.A.P. Ribeiro, A. Camilo, S.R. de Lazaro, Electronic structure and magnetism of new ilmenite compounds for spintronic devices: $FeBO_3$ (B= Ti, Hf, Zr, Si, Ge, Sn), J. Magnet. Magnet. Mater. 394 (2015) 463–469.
[9] Z. Chen, T. Li, T. Yang, H. Xu, R. Khenata, Y. Gao, X. Wang, Palladium (III) fluoride bulk and $PdF_3/Ga_2O_3/PdF_3$ magnetic tunnel junction: multiple spin-gapless

semiconducting, perfect spin filtering, and high tunnel magnetoresistance, J. Nanomater. 9 (9) (2019) 1342, https://doi.org/10.3390/nano9091342.
[10] S.A. Wolf, D. Treger, Spintronics: A new paradigm for electronics for the new millennium, J IEEE Trans. Magnet. 36 (5) (2000) 2748–2751.
[11] R.A. de Groot, F.M. Mueller, P.G.V. Engen, K.H.J. Buschow, New class of materials: half-metallic ferromagnets, J. Phys. Rev. Lett. 50 (25) (1983) 2024–2027.
[12] F. Ahmadian, A. Boochani, Half-metallic properties of the $Co_2Ti_{1-x}Fe_xGa$ Heusler alloys and $Co_2Ti_{0.5}Fe_{0.5}Ga$ (001) surface, Physica B 406 (14) (2011) 2865–2870.
[13] A. Bakhshayeshi, M.M. Sarmazdeh, R.T. Mendi, A. Boochani, First-principles prediction of electronic, magnetic, and optical properties of Co_2MnAs Full-Heusler half-metallic compound, J. Electron. Mater. 46 (4) (2017) 2196–2204.
[14] R. Prakash, G. Kalpana, Prediction of structural, electronic and magnetic properties of full Heusler alloys Ir2YSi (Y= Sc, Ti, V, Cr, Mn, Fe Co, and Ni) via first-principles calculation, J. AIP Adv. 11 (1) (2021) 015042, https://doi.org/10.1063/9.0000101.
[15] H. Masumoto, K. Watanabe, S. Ohnuma, New compounds of the Cl_b, Cl Types of IrMnSb and PdMnTe, new $L2_1$(Heusler) Type of Ir_2MnGa alloys, and magnetic properties, J. Phys. Soc. Jpn. 32 (2) (1972).
[16] H. Masumoto, K. Watanabe, New compounds of the Cl_b, Cl Types of RhMnSb, IrMnSn and IrMnAl, New $L2_1$ (Heusler) type of Ir_2MnAl and Rh_2MnAl alloys, and magnetic properties, J. Phys. Soc. Jpn. 32 (1) (1972).
[17] N. Arikan, H.Y. Ocak, G. Dikici Yıldız, Y.G. Yıldız, R. Ünal, Investigation of the mechanical, electronic and phonon properties of X_2ScAl (X= Ir, Os, and Pt) Heusler compounds, J. Korean Phys. Soc. 76 (10) (2020) 916–922.
[18] E.G. Özdemir, E. Eser, Z. Merdan, Investigation of structural, half-metallic and elastic properties of a new full-Heusler compound–Ir_2MnSi, Chin. J. Phys. 56 (4) (2018) 1551–1558.
[19] G. Forozani, F. Karami, M. Moradi, Structural, electronic, magnetic and vibrational properties of full-Heusler Ir_2CrX (X= Si, Ge) compounds, J. Acta Physica Polonica A 137(3) (2020).
[20] M. Gillessen, Uber die quantenchemischen Untersuchungen einiger ternärer intermetallischer Verbindungen. 2009, PhD thesis, RWTH Aachen.
[21] P. Giannozzi, et al., QUANTUM ESPRESSO: a modular and open-source software project for quantum simulations of materials, J. Phys.: Condens. Mat. 21 (39) (2009), 395502.
[22] https://www.quantum-espresso.org/. [cited 2022 10.03.2022].
[23] J.P. Perdew, K. Burke, M. Ernzerhof, Generalized gradient approximation made simple, J. Phys. Rev. Lett. 77 (18) (1996) 3865–3868.
[24] M. Methfessel, A.T. Paxton, High-precision sampling for Brillouin-zone integration in metals, J. Phys. Rev. B 40 (6) (1989) 3616–3621.
[25] S. Baroni, S. de Gironcoli, A. Dal Corso, P. Giannozzi, Phonons and related crystal properties from density-functional perturbation theory, J. Rev. Modern Phys. 73 (2) (2001) 515–562.
[26] S. Baroni, P. Giannozzi, A. Testa, Green's-function approach to linear response in solids, J. Phys. Rev. Lett. 58 (18) (1987) 1861–1864.
[27] K. Bougherara, F. Litimein, R. Khenata, E. Uçgun, H.Y. Ocak, Ş. Uğur, G. Uğur, AliH. Reshak, F. Soyalp, S.B. Omran, Structural, elastic, electronic and optical properties of Cu_3TMSe_4 (TM= V, Nb and Ta) sulvanite compounds via first-principles calculations, J. Sci. Adv. Mater. 5 (1) (2013) 97–106.
[28] F. Benzoudji, et al., Insight into the structural, elastic, electronic, thermoelectric, thermodynamic and optical properties of MRhSb (M= Ti, Zr, Hf) half-Heuslers from ab initio calculations, J. Chinese J. Phys. 59 (2019) 434–448.
[29] R. Khenata, et al., First-principles calculations of the elastic, electronic, and optical properties of the filled skutterudites $CeFe_4P_{12}$ and $ThFe_4P_{12}$, J. Phys. Rev. B 75 (19) (2007), 195131.
[30] A. İyigör, M. Özduran, M. Ünsal, O. Örnek, N. Arıkan, Ab-initio study of the structural, electronic, elastic and vibrational properties of HfX (X= Rh, Ru and Tc), J. Philos. Mag. Lett. 97 (3) (2017) 110–117.
[31] A.H. Reshak, M.Y. Shalaginov, Y. Saeed, I.V. Kityk, S. Auluck, First-principles calculations of structural, elastic, electronic, and optical properties of perovskite-type $KMgH_3$ crystals: novel hydrogen storage material, J. Phys. Chem. B 115 (12) (2011) 2836–2841.
[32] S. Al, Elastic and thermodynamic properties of cubic perovskite type $NdXO_3$ (X=Ga, In), Eur. Phys. J. B 94 (5) (2021) 108.
[33] G. Murtaza, S.K. Gupta, T. Seddik, R. Khenata, Z.A. Alahmed, R. Ahmed, H. Khachai, P.K. Jha, S. Bin Omran, Structural, electronic, optical and thermodynamic properties of cubic $REGa_3$ (RE=Sc or Lu) compounds: ab initio study, J. Alloy. Compd. 597 (2014) 36–44.
[34] D.G. Pettifor, Theoretical predictions of structure and related properties of intermetallics, J. Mater. Sci. Technol. 8 (4) (1992) 345–349.
[35] N. Arıkan, O. Örnek, Z. Charifi, H. Baaziz, Ş. Uğur, G. Uğur, A first-principle study of Os-based compounds: Electronic structure and vibrational properties, J. Phys. Chem. Solids 96-97 (2016) 121–127.
[36] S. Al, Investigations of Physical Properties of $XTiH_3$ and Implications for Solid State Hydrogen Storage, Zeitschrift für Naturforschung A. 74 (11) (2019) 1023–1030.
[37] I.N. Frantsevich, F.F.V., S.A. Bokuta, Elastic constants and elastic moduli of metals and insulators, ed. I.N. Frantsevich. 1983, Kiev: Naukova Dumka.
[38] J. Haines, J. Leger, G. Bocquillon, Synthesis and design of superhard materials, J. Ann. Rev. Mater. Res. 31 (2001) 1.
[39] J.E. Saal, S. Kirklin, M. Aykol, B. Meredig, C. Wolverton, Materials design and discovery with high-throughput density functional theory: the open quantum materials database (OQMD), J. Jom 65 (11) (2013) 1501–1509.
[40] M. Gilleßen, Informatik und Naturwissenschaften der RWTH Aachen University zur Erlangung des akademischen Grades eines Doktors der Naturwissenschaften genehmigte Dissertation, Von der Fakultat fur Mathematik, 2009.
[41] S. Krishnaveni, M. Sundareswari, M. Rajagopalan, Prediction of electronic and magnetic properties of full Heusler Alloy–Ir_2CrAl, J. Appl. Phys. 7 (2015) 52–55.
[42] A. Jain, S.P. Ong, G. Hautier, W. Chen, W.D. Richards, S. Dacek, S. Cholia, D. Gunter, D. Skinner, G. Ceder, K.A. Persson, Commentary: The Materials Project: a materials genome approach to accelerating materials innovation, APL Materials 1 1 (1) (2013) 011002, https://doi.org/10.1063/1.4812323.
[43] S. Al, M. Yortanlı, E. Mete, Lithium metal hydrides (Li_2CaH_4 and Li_2SrH_4) for hydrogen storage; mechanical, electronic and optical properties, Int. J. Hydrogen Energy 45 (38) (2020) 18782–18788.
[44] B. Fadila, M. Ameri, D. Bensaid, M. Noureddine, I. Ameri, S. Mesbah, Y. Al-Douri, Structural, magnetic, electronic and mechanical properties of full-Heusler alloys Co_2YAl (Y=Fe, Ti): First principles calculations with different exchange-correlation potentials, J. Magn. Magn. Mater. 448 (2018) 208–220.
[45] F. Parvin, et al., First-principles calculations to investigate mechanical, optoelectronic and thermoelectric properties of half-Heusler p-type semiconductor BaAgP, Results Phys. 23 (2021), 104068.